# NASA TECHNICAL MEMORANDUM

NASA TM-73808

NASA TM-73808

(NASA-TM-73808) POTENTIAL DAMAGE TO DC SUPERCONDUCTING MAGNETS DUE TO THE HIGU FREQUENCY ELECTROMAGNETIC WAVES (NASA) 10 p HC A02/MF A01 CSCL 09C

N78-1333

Unclas

G3/33 55205

# POTENTIAL DAMAGE TO DC SUPERCONDUCTING MAGNETS DUE TO HIGH FREQUENCY ELECTROMAGNETIC WAVES

G. J. Gabriel
University of Notre Dame
Notre Dame, Indiana 46556

and

J. A. Burkhart
Lewis Research Center
Cleveland, Ohio 44135



TECHNICAL PAPER to be presented at the
Seventh Symposium on Engineering Problems of Fusion Research
sponsored by the Institute of Electrical and Electronics Engineers
Knoxville, Tennessee, October 25-28, 1977

**NASA TECHNICAL MEMORANDUM**

NASA TM-73808

NASA TM-73808

# POTENTIAL DAMAGE TO DC SUPERCONDUCTING MAGNETS DUE TO HIGH FREQUENCY ELECTROMAGNETIC WAVES

G. J. Gabriel
University of Notre Dame
Notre Dame, Indiana 46556

and

J. A. Burkhart
Lewis Research Center
Cleveland, Ohio 44135

TECHNICAL PAPER to be presented at the
Seventh Symposium on Engineering Problems of Fusion Research
sponsored by the Institute of Electrical and Electronics Engineers
Knoxville, Tennessee, October 25-28, 1977

# POTENTIAL DAMAGE TO DC SUPERCONDUCTING MAGNETS DUE TO HIGH FREQUENCY ELECTROMAGNETIC WAVES*

G. J. Gabriel
Dept. of Electrical Engineering
University of Notre Dame
Notre Dame, IN 46556

J. A. Burkhart
NASA Lewis Research Center
Cleveland, OH 44135

Abstract

Experimental data are presented in support of the hypothesis that a DC superconducting magnet coil does not behave strictly as an inductor, but as a complicated electrodynamic device capable of supporting electromagnetic waves. Travel times of nanosecond pulses and evidence of sinusoidal standing waves have been observed on a prototype four-layer solenoidal coil at room temperature. Ringing observed during switching transients appears as a sequence of multiply reflected square pulses whose durations are related to the layer lengths. With sinusoidal excitation of the coil, the voltage amplitude between a pair of points on the coil exhibits maxima at those frequencies such that the distance between these points is an odd multiple of half wavelength in free space. The voltage amplitude at the lowest order maximum is three times that of the input voltage. Such behavior is typical of wave propagation and agrees with a preliminary analysis based on waveguide theory. The above findings have direct bearing on coil protection in light of experimental evidence of interlayer voltage breakdown. One common scheme of protecting superconducting magnets against excessive ohmic heating due to quenches is to disconnect the power supply according to a prescribed threshold terminal voltage, while a resistor is shunted across the coil to limit the reverse voltage induced by collapse of the magnetic field. This scheme, however, is founded on the circuit theory of inductors and as such ignores the spatial distribution of voltages and currents, a problem which lies in the realm of electrodynamic field theory. Our evidence indicates that any disturbance, such as that resulting from switching or sudden fault, initiates multiple reflections (electromagnetic wave instabilities) between layers, thus raising the possibility for sufficiently high voltages to cause breakdown. Such events occur during the first few microseconds of the normal exponential decay whose duration can be of the order of seconds.

## I. Introduction

Protection of superconducting coils against damage is a problem of major concern to designers of large superconducting magnets (SCM), such as might be employed in thermonuclear fusion and magnetohydrodynamic generators. Excessive ohmic heating due to sudden quenches potentially can damage the cryogenic system as well as the superconductor itself. To protect the magnet during a quench or a fault, one conventional scheme[1,2] is to disconnect the power supply at a threshold terminal voltage. Since the subsequent collapse of the magnetic field can induce transient high voltages, a limiting resistor is shunted across the coil. Theoretically, this resistor should diminish the rate of collapse, as well as dissipate the stored magnetic energy. Despite such a protective measure, evidence of dielectric breakdown has been observed upon disassembling a superconducting solenoid at NASA Lewis Research Center. Conventional circuit analysis, using an inductor representation of this coil and the appropriate value of the protection resistor, predicts voltages insufficient to cause the observed dielectric breakdown. The need for a different approach, therefore, became apparent.

*Research supported by NASA Office of Aeronautics and Space Technology and conducted at the NASA Lewis Research Center during the summer of 1977.

The problem with the conventional scheme is that it is founded on the assumption that a large coil responds as a set of two terminal lumped inductors encountered in circuit theory. As such, circuit theory deals with terminal relations, and does not include the spatial distribution of voltages and currents, which properly falls in the realm of electrodynamic field theory. In the circuit theoretic viewpoint, all events occur simultaneously, or in phase, at all points along the coil. Yet, from a field theoretic standpoint, a resistor placed at the terminals of a coil serves merely as a boundary constraint, but the timing of voltages may differ from point to point, and their magnitudes within the coil might even exceed that of the terminal voltage.

This paper presents experimental data, together with a preliminary theoretical analysis, in support of the hypothesis that a large superconducting coil does not behave as a simple inductor, but as a complicated electrodynamic device capable of supporting propagating electromagnetic waves. This represents a first attempt at a field theoretic approach to the problem of protecting superconducting coils. The results are preliminary in nature, and indicate that the key to devising protective methods and analytical models might lie in an understanding of the electrodynamics of the coil as a wave-guiding structure.

The first attempts of an experimental test of the hypothesis were made on one of the superconducting solenoids of the NASA Superconducting Magnetic Mirror Apparatus (SUMMA)[3,4]. Confirmation of the existence of a multiplicity of resonances on this magnet, operated at both LHe and room temperatures, motivated further exploration of the phenomena on a four-layer prototype coil at room temperature, whose choice was dictated by the need for flexibility. For macroscopic fields, the primary difference between the two coils is the significantly lower wave attenuation (damping) in the superconducting one, a circumstance which enhances some of the effects observed in the normal prototype coil. The experimental data on this coil are presented in Section II, followed by a theoretical interpretation in Section III.

## II. Experimental Results

A photograph of the prototype coil, measuring 12" in diameter and 12" in axial length, is shown in Fig. 1. It is composed of four solenoidal layers each with 135 turns of Formvar-insulated copper-clad Nb-Ti wire.

This layer-wound coil was constructed of the same wire and used the same layer-to-layer spacing as the previously tested SUMMA coil. The length, L, of the wire in the four spiral layers is approximately 525 meters. As it will become evident, this length plays an important role in the dynamic behavior of the coil.

As in the SUMMA superconducting coils, each pair of layers in the four-layer coil exhibits one resonance (where input current is minimum) at low frequencies (< 25 kHz) in addition to high-frequency resonances periodically spaced in the frequency domain. This low-frequency resonance does not correlate well with the frequencies calculated by circuit theory using the measured interlayer capacitances and layer inductances. However, placement of an aluminum foil sheet within the coil bore at the inner circumference of the coil (to simulate a mandrel) did shift the resonance from 13.7 kHz to 22.5 kHz as one might expect qualitatively from circuit theory. Yet this simulated mandrel had no effect on the high-frequency behavior of the coil. Further, the low-frequency resonance bears no discernible relation to the high-frequency behavior of the coil under switching transients. Under such transients the low-frequency resonance was successfully suppressed by the addition of a damping resistor shunted across the coil terminals. However, this resistor did not eliminate the high-frequency ringing. Thus from the standpoint of coil protection, the low frequency phenomena do not pose serious problems. Excessively high interlayer voltages appear to be the result of high frequency traveling waves.

1. Standing Wave Resonance

The voltage $V_{12}$ between the junctions of paired layers, corresponding to distances L/4 and 3L/4 along the coil, were measured in the circuit configuration shown in Fig. 2a, with sine wave excitation. The oscilloscope trace in Fig. 2b was obtained by electronic sweep of the frequency between 0.1 and 10 MHz, while the graph in Fig. 2c was obtained manually. The amplitude of $|V_{12}|$ at the first peak is 3.8 times that of the input terminal voltage. This is a significant datum because it clearly shows that voltages within the coil can exceed its terminal voltage.

The spacing between maxima and minima in Fig. 2c appears to be related to the ratio of the coil length, L, to the free-space wavelength, $\lambda$, of the input signal. The maxima of $|V_{12}|$ occur at those frequencies when the distance L/2, between the sampled junctions is 0.52$\lambda$, 1.6$\lambda$, 2.88$\lambda$... This relation closely resembles the sequence $L/2 = \lambda/2, 3\lambda/2, 5\lambda/2$, which is usually encountered when standing waves exist on any waveguide structure. This behavior clearly indicates that the electromagnetic field travels, in part, along the spiral path of the coil.

2. Pulse Transit Time

The balanced configuration shown in Fig. 3a was employed to measure the time of travel of electromagnetic disturbances along the coil. The upper trace in Fig. 3b shows the pulse at J1 to be delayed by 400 nsec, relative to the input pulse at J12, while the inverted pulse at J1 is delayed by 1180 nsec, or roughly three times the delay of the first pulse. Apparently, the positive pulse starting from the positive terminal of the generator travels over one layer, while the negative pulse starting from the negative terminal travels over three layers. The calculated travel time per layer is 430 nsec, based on the speed of light in vacuum. The fragmented pulse at J1 at the onset of the input signal appears to arrive through an axial path (1 nsec) provided by capacitive and inductive coupling between adjacent turns.

3. Multiple Reflection

The response of the coil to a square wave input, in the configuration of Fig. 4a, is shown in the traces in Fig. 4b, while the same trace in expanded scale is shown in Fig. 4c. This pattern is typical of multiple reflections of step functions, providing additional evidence of wave propagation. The duration of each reflected step is approximately 810 nsec which is close to the calculated travel time of 860 nsec over half the coil length. Since contactors and switching devices of real systems might not have the rapid rise and fall times of the square wave generator used for the data of Fig. 4, the coil was manually energized and de-energized to a current level of 5 amperes, dc. Once again a ringing was observed in the first few microseconds of the normal exponential decay. This ringing was analyzed to be a sereis of alternating multiply-reflected-steps having the same durations as shown in Figs. 4b and 4c.

## III. Theoretical Interpretation

The following development from the theory of uniform waveguides is presented as a preliminary frame work in which to interpret the above experimental results, which otherwise cannot be explained strictly by circuit theory. It has been shown[5] that the electromagnetic field along any path, either straight or curved, occupied by a conductor can be described by the Lorentz potentials $\underline{A}$ and $\phi$ satisfying the equations

$$\frac{\partial}{\partial x} A_x(x,t) = -\frac{1}{c^2}\frac{\partial}{\partial t}\phi(x,t) \qquad (1)$$

$$\frac{\partial}{\partial x}\phi(x,t) = -\frac{\partial}{\partial t} A_x(x,t) \qquad (2)$$

where c is the speed of light and x is the distance along the path. These potentials can be related to observable voltages and currents via normalization integrals appropriate to the geometry of the conductor path. Since these integrals are not easily calculable for a coil at this stage, we appeal to the simple case of a straight wire, even though it is not completely realistic. For this case, the normalization yields

$$\frac{\partial}{\partial x} v(x,t) = -\frac{Z_0}{c}\frac{\partial}{\partial t} i(x,t) \qquad (3)$$

$$\frac{\partial}{\partial x} i(x,t) = -\frac{1}{Z_0 c}\frac{\partial}{\partial t} v(x,t) \qquad (4)$$

where $v(x,t)$ is the voltage along the wire relative to an arbitrary reference, $i(x,t)$ is the current, and $Z_0$ is the characteristic wave impedance.

The conditions of the experiments on the coil can be represented best by considering excitation of the line by a generator connected between the conventional input-output terminals, as shown in Fig. 5. This configuration imposes the boundary conditions

$$v_s(t) = i_s R_s + v\left(-\frac{L}{2}, t\right) - v\left(\frac{L}{2}, t\right) \qquad (5)$$

$$i_s(t) = i\left(-\frac{L}{2}, t\right) = i\left(\frac{L}{2}, t\right) \qquad (6)$$

ORIGINAL PAGE IS OF POOR QUALITY

where $v_s(t)$ and $i_s(t)$ are the generator voltage and current, respectively, and $R_s$ is its internal resistance.

Employing the convenience afforded by Laplace Transforms, and denoting such transforms by underscores, e.g., $\underline{u}(x,s)$, we find the solution to Eqs. (3) and (4) subject to the conditions (5) and (6) to be

$$\underline{v}(x,s) = \frac{\underline{v}_s(s)}{z_s + 1} e^{-sL/2c} \frac{\sinh(sx/c)}{1 + \Gamma_s e^{-sL/c}} \quad (7)$$

$$\underline{i}(x,s) = \frac{1}{Z_0} \frac{\underline{v}_s(s)}{z_s + 1} e^{-sL/2c} \frac{\cosh(sx/c)}{1 + \Gamma_s e^{-sL/c}} \quad (8)$$

where $z_s = R_s/2Z_0$ and

$$\Gamma_s = \frac{z_s - 1}{z_s + 1}$$

$\Gamma_s$ is the reflection coefficient of the generator. It is worth noting that, at the midpoint of the line, $\underline{v}(0,s)$ is always zero regardless of the reference, while at the end points the voltages are equal and of opposite sign. Consequently, the midpoint may be taken properly as the voltage reference.

1. Standing Wave Resonance

In order to interpret the results in Section II-1, it is necessary to express the voltages and currents in complex phasor representation appropriate to sinusoidal excitation. This may be done directly by the substituion $s = j\omega$ in Eqs. (7) and (8), where $\omega$ is the angular frequency. The quantity of interest is $|V_{12}|$ which is given by

$$|V_{12}| = \left|\underline{v}\left(-\frac{L}{4}, j\omega\right) - \underline{v}\left(\frac{L}{4}, j\omega\right)\right| . \quad (9)$$

Carrying out the algebraic operations we find $|V_{12}|$ to be

$$|V_{12}| = \frac{|V_s|}{z_s + 1} \frac{2}{g} |\sin(\omega L/4c)| \quad (10)$$

and the input current amplitude to be

$$|I_s| = \frac{|V_s|}{z_s + 1} \frac{1}{Z_0 g} |\cos(\omega L/2c)| \quad (11)$$

where

$$g = \left[1 + \Gamma_s^2 + 2\Gamma_s \cos(\omega L/c)\right]^{1/2}.$$

Equations (10) and (11) are plotted in Fig. 6 for $\Gamma_s = -0.5$, for the purpose of illustration. It is seen that the voltage exhibits maxima at the frequencies

$$f_n = (2n + 1)\ c/L,\ n = 0,1,2,...$$

while the input current has its maxima at

$$f_m = mc/L,\ m = 1,2,...$$

The maxima shift according to whether $\Gamma_s$ is positive or negative, which is determined by the ratio $z_s$.

For the four-layer coil, with L = 525 meter, the theoretical frequencies for voltage maxima would be

$$f_n = 0.571,\ 1.71,\ 2.85\ \text{MHz}$$

compared to the observed values of 0.6, 1.85, 3.4 MHz. As to be expected, the theory of uniform lines is not adequate quantitatively. Nevertheless, it illustrates that the observed phenomena are not the result of circuit theoretic resonance but due to standing waves in space.

2. Pulse Travel Time

To interpret the delay times indicated in Fig. 3, we note that $v_{J12}(t)$ and $v_{J1}(t)$ correspond to

$$\underline{v}_{J12}(s) = \underline{v}\left(-\frac{L}{2}, s\right) \quad (12)$$

$$\underline{v}_{J1}(s) = \underline{v}\left(-\frac{L}{4}, s\right). \quad (13)$$

By applying the Laplace inversion to Eq. (7) evaluated at x = - L/2, - L/4, one finds

$$v_{J12}(t) = \frac{1}{z_s + 1} \sum_{n=0}^{\infty} (-\Gamma_s)^n \times \left\{v_s(t - 4n\tau) - v_s\left[t - 4(n + 1)\tau\right]\right\} \quad (14)$$

$$v_{J1}(t) = \frac{1}{z_s + 1} \sum_{n=0}^{\infty} (-\Gamma_s)^n \times \left\{v_s\left[t - (4n + 1)\tau\right] - v_s\left[t - (4n + 3)\tau\right]\right\} \quad (15)$$

where $\tau = L/4c$. A sketch of the first terms (n = 0) of $v_{J12}$ and $v_{J1}$ is shown in Fig. 7 for an arbitrary input pulse $v_s$. The higher order terms diminish as $\Gamma_s^n$. Comparing this sketch to the observed trace in Fig. 3b shows that the agreement between theory and experiment is excellent in this case.

## IV. Conclusion

We have presented experimental data which, when interpreted in the framework of the theory of waves on straight wires, demonstrate that a large coil behaves as a straight waveguide structure. From the standpoint of coil protection, it is significant that voltages between layers within a coil were found to differ from and even exceed those measured at terminals where protective resistors are usually placed. Such resistors were found to suppress the low-frequency oscillation, but not the high-frequency multiple reflections and standing waves. Since the characteristic impedance of a waveguiding structure plays a decisive role in the multiple reflections which cause these high-frequency resonances, the solution for coil protection against excessive voltages and, for that matter, against any random stimulation of undesired oscillations might well lie in impedance matching at selected points throughout the coil system.

ORIGINAL PAGE IS
OF POOR QUALITY

While the motivation for this research was better understanding of the dielectric breakdown in superconducting magnets, the wave phenomenon discovered has broader implications. Since multiple reflections can be stimulated by a random disturbance, switching transient, or sudden fault, these oscillating waves constitute an instability capable of transforming the energy of a quiescent dc superconducting coil into dissipative ac energy, even when dielectric breakdown does not occur.

The findings also illustrate the inadequacy of viewing a coil only as a lumped inductor. Even the representation by sections of distributed inductances and capacitances, such as has been attempted for power transformers[6,7], is questionable because there are no a priori criteria by which one decides the number of needed sections and by which one justifies the assumed topology of interconnections. In light of the rudimentary theory presented here, a thorough field theoretic analysis of coils in general appears desirable and deserving of the effort.

## References


1. Maddock, B. J. and James, G. B.: Protection and Stabilization of Large Superconducting Coils, Proc. IEE, 1968, Vol. 115, No. 4, pp. 543-547.

2. Thome, R.J. and Ayers, J. W.: Design Study of Superconducting Magnets for a Combustion Magnetohydrodynamic (MHD) Generator, NASA CR-135178. 1977.

3. Reinmann, J. J., Patch, R. W.; Lauver, M. R.; Englert, G. W.; and Snyder, A.: SUMMA Hot-Ion Plasma Heating Research at NASA Lewis Research Center, Proc. Sixth Symp. Eng. Problems of Fusion Research, IEEE Pub. No. 75CH1097-5-NPS, 1975, pp. 423-429.

4. Reinmann, J. J.; Swanson, M. C.; Nichols, C. R.; Obloy, S. J.; Nagy, L. A.; and Brady, F.J.: NASA Superconducting Magnetic Mirror Facility, Proc. Fifth Symp. Eng. Problems of Fusion Research, IEEE Pub. No. 73CH0843-3-NPS, 1973, pp. 587-591.

5. Gabriel, G. J.: Relativistic Foundations of Wave Transmission Structures, to be published.

6. NcNutt, W. J.; Blalock, T. J.; and Hinton, R. A.: Response of Transformer Windings to System Transient Voltages, Proceedings IEEE Power Engineering Society Meeting and EHV/UHV Conference, July 1973, pp. 457-467.

7. Fergestad, P. I. and Henricksen, T.: Transient Oscillations in Multiwinding Transformers, Proceedings IEEE Power Engineering Society Meeting and EHV/UHV Conference, pp. 500-501, July 1973.

E-9391

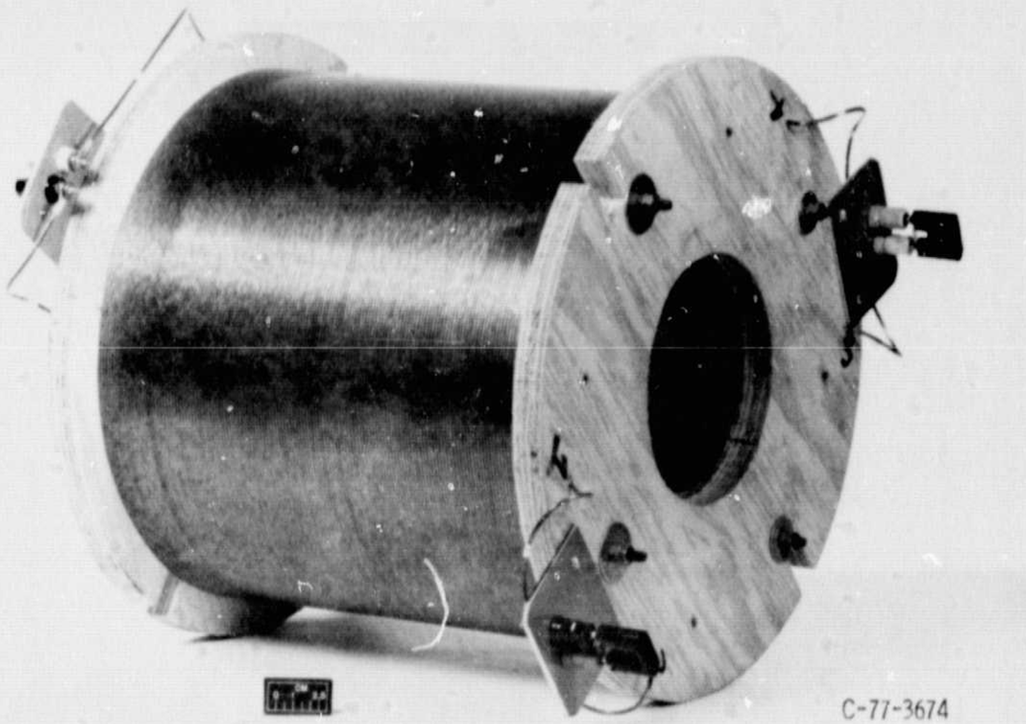

C-77-3674

Figure 1. - Four-layer coil.

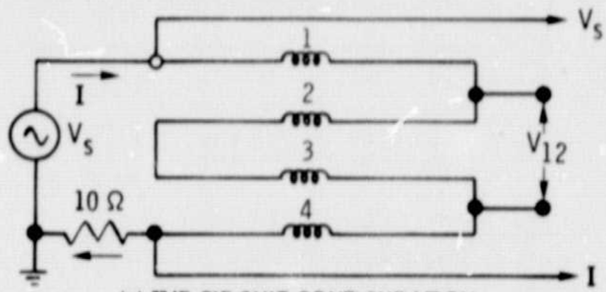


(a) THE CIRCUIT CONFIGURATION.

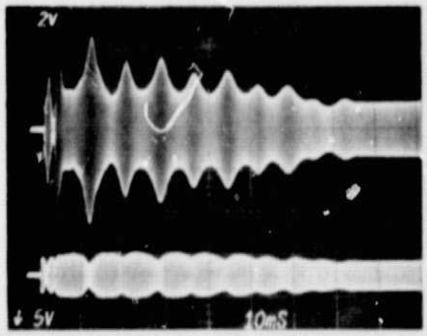


(b) DATA FROM FREQUENCY SWEPT SINUSOIDAL INPUT SHOWING $V_{12}$ IN UPPER TRACE AND $V_s$ IN LOWER TRACE, SCALE = 1.6 MHz/cm.

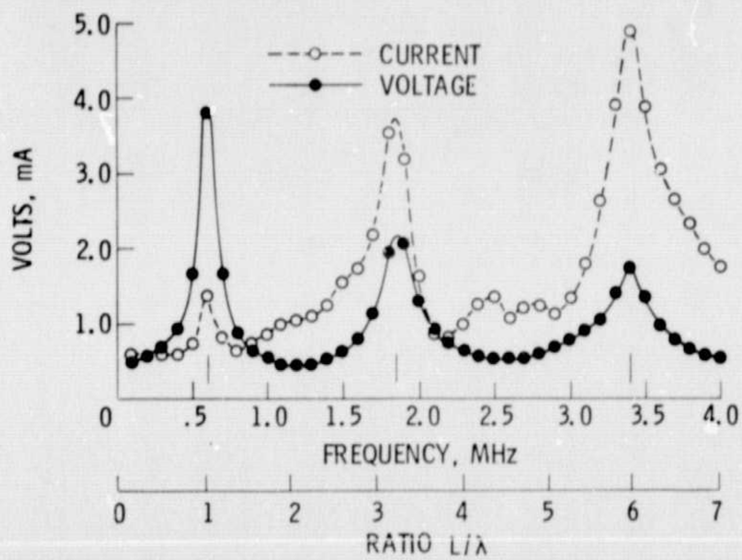


(c) MANUAL PLOT OF $V_{12}$ AND I NORMALIZED TO $V_s$ = 1.0 volt.

Figure 2. - Standing wave resonance.

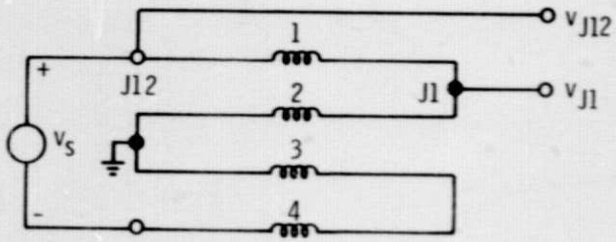


(a) THE CIRCUIT CONFIGURATION.

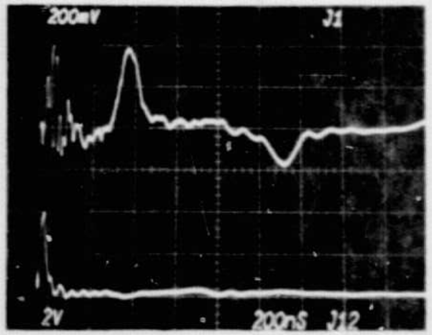


(b) THE OBSERVED TRACE AT J12 AND J1.

Figure 3. - Pulse travel time.

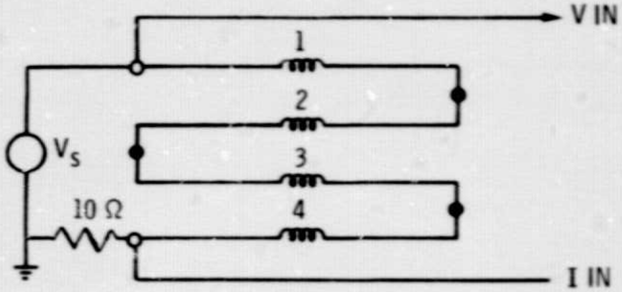


(a) THE CIRCUIT CONFIGURATION.


(b) MULTIPLY REFLECTED STEPS IN THE INPUT CURRENT I, UPPER TRACE, AND THE INPUT VOLTAGE, LOWER TRACE.

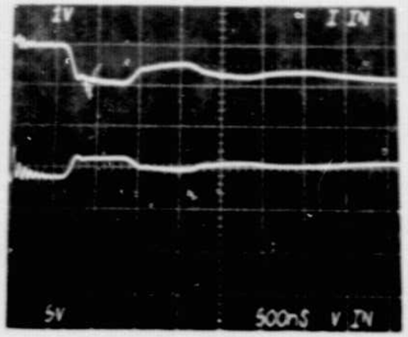


(c) SAME TRACE ON EXPANDED TIME SCALE.

Figure 4. - Square wave response.

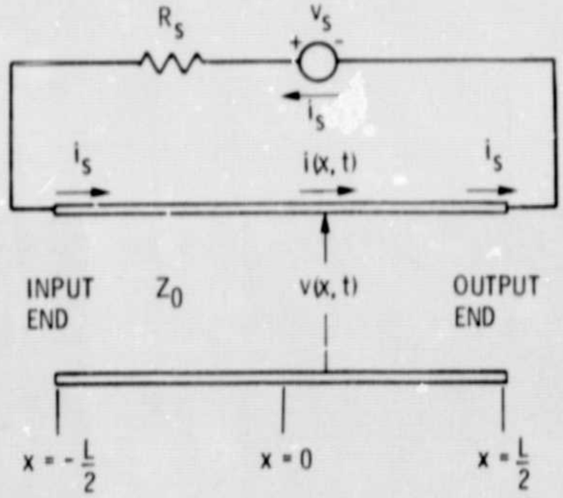


Figure 5. - Straight wire transmission line analogue of coil.

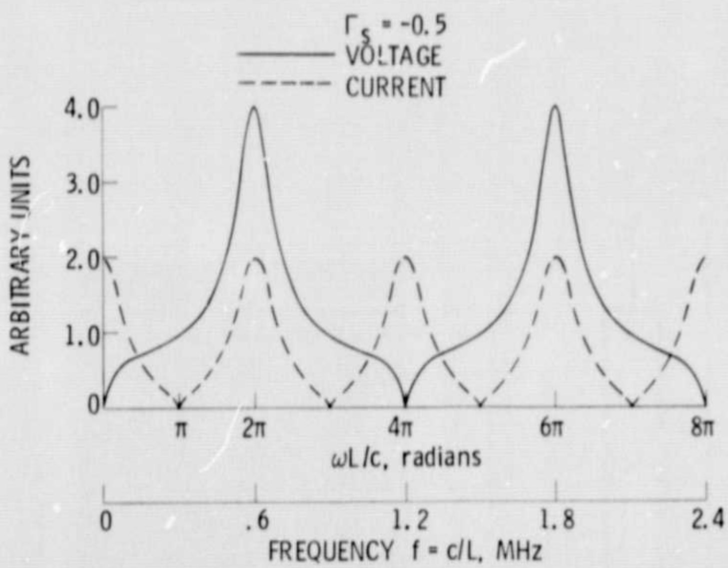


Figure 6. - Theoretical standing wave resonance for straight wire showing the input current and the voltage between $x = + L/4$ and $x = - L/4$ corresponding to $V_{12}$ of figure 2.

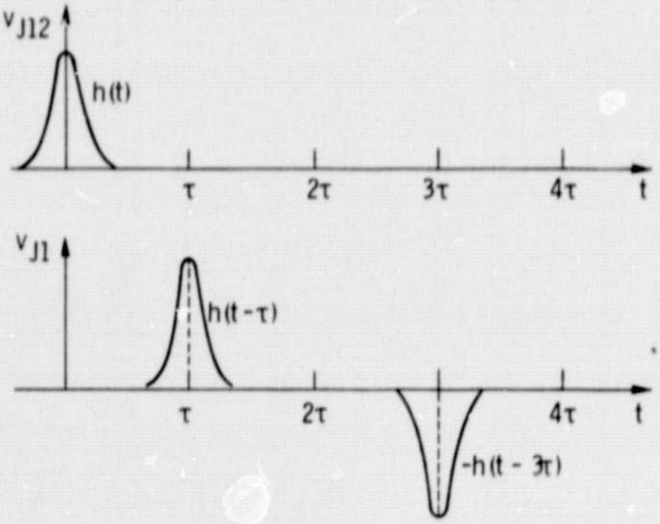


Figure 7. - Theoretical pulse travel times for straight wire.



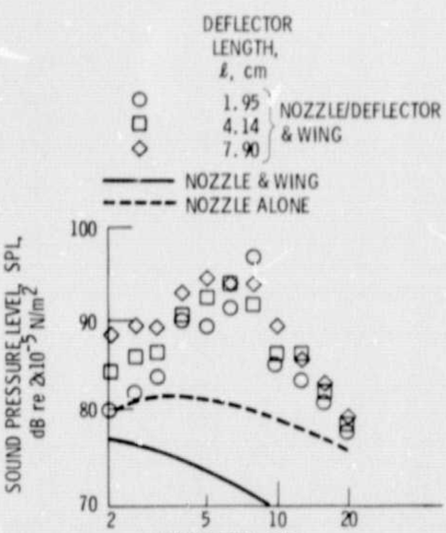


Figure 8. - Variation of deflector spectra with deflector length, ℓ. 3/2-baseline wing; $60^{\circ}$ flap setting; $40^{\circ}$ deflector setting; $M_j$, 0.8; $60^{\circ}$ radiation angle.